

Bispecific Monoclonal Antibody-Mediated Targeting of an Indium-111-Labeled DTPA Dimer to Primary Colorectal Tumors: Pharmacokinetics, Biodistribution, Scintigraphy and Immune Response

Jean-Marc Le Doussal, Alain Chetanneau, Anne Gruaz-Guyon, Marie Martin, Emmanuel Gautherot, Paul-Antoine Lehur, Jean-François Chatal, Michel Delaage and Jacques Barbet

Immunotech SA, Marseille; Service de Médecine Nucléaire, Centre René Gauducheau; and Service de Chirurgie Digestive, Centre Hospitalier Régional, Saint-Herblain, France

Eleven patients with primary colorectal carcinoma tumors (4 ± 2 cm) were given intravenous injections of 1–10 mg of an anti-CEA, anti-In-DTPA bispecific Fab'-Fab monoclonal antibody, and 2–8 days later, were injected with 1.2–4.2 nmol of an ^{111}In -labeled DTPA dimer (6 mCi). The bispecific antibody exhibited good stability and F(ab)'_2 -like pharmacokinetics. After injection, the ^{111}In -DTPA dimer distributed in a large volume (88 ml/kg–180 ml/kg) and cleared through the kidneys (mean residence time in the whole body: 9 hr–16 hr). Uptake of ^{111}In by the tumor using this two-step technique (1.8%–17.5% injected dose ID/kg, measured from surgical samples 48 hr after hapten injection) was not found significantly lower than that achieved with our reference ^{111}In -labeled anti-CEA F(ab)'_2 , 1 to 4 days after injection in six patients with similar clinical status (5.5%–30.2% ID/kg). In addition, tumor-to-blood and tumor-to-liver uptake ratios were significantly improved (blood 7.8 versus 4.2, liver 2.8 versus 0.8). As a result, low background images allowed detection of 12 of 13 lesions, 4 hr and 24 hr after hapten injection. However, 7 of 11 patients developed HAMA.

J Nucl Med 1993; 34:1662–1671

The targeting of radiolabeled, low molecular weight tracers by bispecific monoclonal antibodies (Bs-Mab) with specificity for both a cell-surface tumor-associated antigen and a hapten, has been suggested as an alternative method to use of radiolabeled anti-tumor Mabs for tumor immunoscintigraphy and radioimmunotherapy (1). This pretargeting (or two-step) method has been advocated as affording faster clearance of excess radioactivity, lower nonspecific

background and better purity and stability of the radiolabeled molecules.

Animal experiments have been performed by several investigators (2–4), demonstrating that ^{125}I - or ^{111}In -labeled haptens could be targeted to human tumors grafted in nude mice, provided that the mice were injected earlier with 2 μg amounts of (anti-tumor, anti-hapten) Bs-Mab. Good isotope localization in tumors was obtained with expected improvements of (1) faster uptake by the tumor and (2) accelerated clearance of excess radioactivity from normal tissues (4).

Results were confirmed qualitatively in an immunoscintigraphy study conducted by Stickney et al. (5) in colorectal carcinoma patients, using an (anti-CEA, anti-benzyl-In-EDTA) Bs-Mab and an ^{111}In -labeled benzyl-EDTA-bleomycin derivative as labeled hapten. Although tumor imaging was achieved, high Bs-Mab doses were used (5–40 mg) and a carrier dose of Bs-Mab was coinjected with the labeled hapten.

The use of bivalent haptens (6) was shown to increase the tumor-to-nontumor uptake ratio (UR), while decreasing the Bs-Mab ID needed to achieve maximal hapten uptake by the tumor. Indeed, bivalent haptens exhibit an enhanced affinity for cell-bound Bs-Mab, when compared to free circulating Bs-Mab, as the result of formation of stable cyclic complexes (7) on the cell membrane (8). In addition, the hydrophilic character of bivalent haptens has been shown a prerequisite for in vivo use (9).

A clinical study was conducted in 11 patients with primary colorectal tumor with known tumor location, using a hydrophilic ^{111}In -labeled bivalent DTPA derivative and an (anti-CEA, anti-In-DTPA) Bs-Mab. We studied patient tolerance and immune response to Bs-Mab; the pharmacokinetics of the Bs-Mab and of the hapten; the biodistribution of the hapten in tumor and in normal tissues (compared with that obtained with ^{111}In -labeled F(ab)'_2 in six patients

Received Apr. 27, 1992; revision accepted May 25, 1993.

For correspondence and reprints contact: Jean-Marc Le Doussal, PhD, Immunotech SA, 130 Avenue De Lattre de Tassigny, BP 177, 13276 Marseille Cedex 9, France.

with similar clinical status); the efficacy of the tumor imaging method; and the influence of Bs-Mab ID, hapten ID and timing of injections on the pharmacokinetics of the Bs-Mab and of hapten, on the biodistribution of the hapten, and the quality of the images.

PATIENTS, MATERIALS AND METHODS

Patients

Eleven patients with colon adenocarcinoma detected by colonoscopy were admitted to the study after giving written informed consent. Table 1 summarizes their relevant clinical characteristics. The ^{111}In -labeled F(ab)_2 protocol was performed in six patients with similar clinical status.

Mab, Fragments and Bs-Mab

Anti In-DTPA clone 734.19.22 (abbreviated 734) that secretes a mouse monoclonal IgG_1 (μIgG_1), lambda chain, specific for In-DTPA complexes, was obtained as previously described (4).

Maleimide derivatized 734 Fab was obtained from concentrated cell culture supernatants by centrifugation, immobilization on a DTPA-calcium derivatized gel, fragmentation with papain in the presence of 50 mM of cysteine, washing, elution with 0.1 M ethylenediaminetetraacetic acid (EDTA) buffered to pH 3.8 with NaOH, extensive dialysis against 20 mM HEPES buffer, 0.15 M NaCl, pH 7.5, concentration to 10 mg/ml, blockade of residual thiol activity with a three-fold molar excess of *N*-ethyl-maleimide and reaction with the same excess of *e*-maleimidocaproic acid, *N*-hydroxysuccinimide ester.

Sterile and nonpyrogenic F(ab)_2 and DTPA-derivatized F(ab)_2 (10) of the F6 monoclonal μIgG_1 , kappa chain, specific for human carcinoembryonic antigen (11), were provided by Dr J. C. Saccavini (Cis Biointernational, Gif sur Yvette, France). F6 F(ab)_2 (10 mg/ml in 0.1 M phosphate buffer, pH 6.0) was reduced for 1 hr at 37°C in the presence of 10 mM cysteamine.

The reduced F6 Fab' and the EMCS-derivatized 734 Fab were separated from excess cysteamine or EMCS by size exclusion chromatography on a Superdex column (Pharmacia, Uppsala, Sweden) using 20 mM HEPES buffer, 0.15 M NaCl, pH 7.5, pooled in an equimolar ratio, concentrated to 10 mg/ml and allowed to react overnight at room temperature. Bs-Mab with an apparent molecular weight of 100,000 Da was separated from nonreacted Fab and Fab' on a Superdex column as described above.

DTPA- F(ab)_2 F6 (1 mg) was labeled with 3 mCi of $^{111}\text{InCl}_3$ as previously described (11). F6 DTPA- F(ab)_2 labeling yield was measured by thin-layer chromatography (12).

Synthesis of Indium-111 Labeled *N*-ε-(In-DTPA)-tyrosyl-*N*-ε-(In-DTPA)-lysine: Indium-111-di-(In-DTPA)-TL

Di-(In-DTPA)-TL was obtained (4) after reaction of DTPA dianhydride with tyrosyl-lysine diacetate, purification by size exclusion chromatography and by reverse-phase chromatography. The final product was dissolved at 2.5 μM in a 0.1 M acetate, 10 mM citrate buffer, pH 5.0. Di-DTPA-TL solution (2.5 nmol (1 ml)) was added to 6 mCi of ^{111}In -chloride (Cis Biointernational, 10 mCi/ml in 50 mM HCl). Chelation was performed overnight at room temperature. Then, 100 nmol of unlabeled InCl_3 was added and allowed to saturate free chelating groups for 1 hr. For Patient 11, a 2.5-nmol dose of nonradioactive Di-(In-DTPA)-TL was added to the labeled hapten before injection. Indium-111 immunoreactivity for anti-(In-DTPA) Mab was checked before injection

by incubating the adequate dilution of labeled hapten in 734-IgG-coated tubes for 1 hr at room temperature.

Bs-Mab Protocol

Patients were intravenously given a 30-min Bs-Mab infusion (0.9–9 mg in 100 ml of NaCl 9 g/liter) 8–2 days before hapten injection. At day 0, they were injected intravenously with 5–8 mCi of ^{111}In -di-(In-DTPA)-TL diluted in 5 ml of a 9 g/liter NaCl solution. Individual protocols are detailed in Table 1. Six hours later, after the first image acquisition sequence, they received an intravenous injection of 10 mCi of $^{99\text{m}}\text{Tc}$ -labeled hydroxy-methylene-diphosphonate (HMDP, Cis Biointernational).

Serum samples were taken before Bs-Mab injection, before hapten injection and 5 min, 30 min, 1 hr, 5 hr, 24 hr, 48 hr, 3 wk and 1.5 mo after hapten injection. Urine was collected between 0–5 hr and 5–24 hr after hapten injection. At Day 2 (Day 3 for Patient 10), patients underwent surgery. The tumors were resected and biopsies of muscle, skin, fat and liver were taken.

Image acquisition sequences were performed 4 hr and 24 hr after hapten injection, consisting of a whole-body scan (20 min using a Scanicamera, CGR, France equipped with low-energy collimators and tuned to a 210 keV energy peak with a 60% window), two static abdominal views (posterior and anterior, 10 min each, using a Sophycamera DS7 from Sopha Medical, France, a medium-energy collimator, tuned to 173 and 247 keV energy peaks with 20% windows for ^{111}In and the 140 keV peak with 15% windows for $^{99\text{m}}\text{Tc}$) and a 40-min tomographic acquisition with the same camera (64 steps, reconstructed using the Wiener filter with a Sophy 20 P image processing system). Patients were asked to urinate before imaging.

CEA serum levels before Bs-Mab injection were determined with the immunoradiometric kits obtained from Cis Biointernational, as described by the manufacturer.

Human anti-Bs-Mab concentration was determined in serum by a one-step sandwich RIA with F6-734 Bs-Mab on the solid phase and ^{125}I -labeled F6-734 Bs-Mab as tracer. Serial dilutions of an anti- μIgG goat polyclonal antibody (GAMIG, Immunotech, Marseille, France) in a pool of normal human sera were used as reference.

The fine specificity of anti-Bs-Mab response was evaluated after addition of 3 μg of F6-734 Bs-Mab, 734 Fab, F6 Fab' and a 1:1 mixture of both Fab and a 1:1 mixture of irrelevant mouse Mab IgG_1 Fab (one with a kappa light chain, one with a lambda light chain).

The isotype of the anti-Bs-Mab response was determined using a two-step sandwich RIA using the same solid phase but ^{125}I -labeled anti-(human IgG , hIgG) or anti-hIgM antibodies (Immunotech) as tracers. Reference curves were obtained by dilution of In-DTPA-derivatized pure hIgG or hIgM in a pool of normal human sera.

μIgG concentrations were measured in serum samples as above, but using GAMIG (reactive with kappa and lambda light chains) on the solid phase and ^{125}I -labeled GAMIG as the tracer. A reference curve was obtained by serial dilutions of purified Bs-Mab in the serum of the same patient collected before Bs-Mab injection. This RIA quantifies Bs-Mab in serum, as well as its possible complexes or fragments (especially F6 and 734 Fab obtained after an eventual Bs-Mab cleavage).

Bs-Mab concentrations were measured under the same conditions with In-DTPA-BSA (4) on the solid phase and an ^{125}I -labeled rat anti-mouse kappa chain (RAMK, Immunotech) as a tracer. The reference curve was obtained as previously described.

TABLE 1
Patient Status and Injection Protocol

Mean ^a /s.d.– \times s.d.			Patient no.										
			1	2	3	4	5	6	7	8	9	10	11
Sex			M	M	M	F	M	F	F	M	F	F	M
Age (yr)			74	57	70	75	70	56	85	58	77	70	67
Serum CEA (normal <6) (ng/ml)			6	2	2	5	29	1	7	3	2	6	4
Dukes stage			A	B	B2	B	B2	B	B2	C	B	C2	A
Tumor site [†]			S	R	LC	S	RC	R	R	R	R	R	RC
Tumor size (cm)			2	7	4	4	5/8	4	3	2/4	5.5	2	1
Tumor volume [‡] (ml)			3	50	30	40	90/80	35	12	8/na	30	8	1
Tumor CEA expression			+++	+	++	+++	++	++	++	++	+++	++	na
Body weight (kg)			74	82	74	42	70	46	33	92	47	61	75
Bs-Mab injected dose (mg)	3.1	1.4–7.0	4.5	0.9	0.9	4.5	4.5	4.5	0.9	4.5	4.5	4.5	9.0
Interval between injections (days)	3.3	2.0–5.5	2.0	2.0	2.0	4.0	2.0	4.0	2.0	8.0	5.0	5.0	5.0
Hapten injected dose (nmol)	2.2	1.6–3.2	1.1	2.2	2.2	2.2	2.2	2.2	2.2	2.2	2.2	2.2	4.5
Mouse IgG and Bs-Mab (italics) pharmacokinetics at the time of tracer injection													
Concentration in plasma (μ g/ml)	1.9	0.9–3.8	2.0	1.0	1.1	4.5	3.7	4.4	0.9	0.6	2.0	1.5	3.8
	1.5	0.7–3.4	2.3	1.0	0.4	3.2	4.3	2.8	1.2	0.4	1.8	1.3	2.6
Distribution volume [§] (ml/kg)	55	22–142	118	31	65	36	19	9	145	235	60	106	48
	85	26–260	na	na	na	63	42	17	190	763	63	65	101
Elimination half-life (hr)	39	23–66	35	26	62	35	15	21	45	107	40	54	44
	56	22–140	na	na	na	40	26	22	188	282	39	38	55
Bs-Mab per mouse IgG [¶] (%)	82	57–118	115	100	36	71	116	64	133	67	90	88	70
¹¹¹ In-di-(In-DTPA)-TL pharmacokinetics in the presence of circulating Bs-Mab													
Vc ^{**} (ml/kg)	61	51–73	50	67	70	64	45	56	79	71	58	69	49
Vss (ml/kg)	126	88–180	74	139	178	126	78	96	192	226	119	137	106
Ftiss (%)	50	41–61	33	52	61	49	43	41	59	69	51	50	53
Ta (min)	29	23–38	29	23	37	22	25	43	37	33	26	22	40
Tb (hr)	19	14–25	25	15	14	24	19	15	15	27	22	31	27
MRTc (hr)	6	4–9	11	5	2	9	7	8	4	4	6	6	8
MRTb (hr)	12	9–16	17	10	6	17	12	14	10	14	13	12	18
Urine recovery after 24 hr (%)	57	41–81	41	86	80	42	54	60	na	90	60	32	60
¹¹¹ In-di-(In-DTPA)-TL biodistribution in surgical samples (%/ID/kg or %/ID/liter)													
Tumor	5.6	1.8–17.5	10.9	1.6	1.2	56.5	4.8	7.4	9.4	1.9	14.5	6.7	2.4
Blood	0.7***	0.3–1.7	2.6	0.5	0.1	1.2	1.2	1.0	0.9	0.4	1.3	1.1	0.3
Colon	2.0***	0.8–5.0	4.2	0.5	0.6	6.3	4.3	2.7	2.4	0.6	4.5	1.3	na
Liver	2.0***	1.2–3.3	2.2	2.8	0.8	3.7	2.4	4.9	1.4	1.5	1.3	2.0	2.0
Muscle	0.2***	0.1–0.5	0.3	0.1	0.1	0.5	na	0.7	0.2	0.1	0.2	0.3	0.2
¹¹¹ In-di-(In-DTPA)-TL uptake ratios at the time of surgery													
Tumor/blood	7.8	3.7–16.6	4.3	3.5	10.8	49.1	4.1	7.6	11.1	4.2	11.5	6.3	8.3
Tumor/colon	3.1	1.8–5.4	2.6	3.2	1.9	9.0	1.1	2.8	3.9	3.2	3.2	5.0	na
Tumor/liver	2.8	1.0–7.7	4.9	0.6	1.4	15.4	2.0	1.5	6.8	1.3	10.8	3.4	1.2
Tumor/muscle	28.6	12.9–63.0	33	15	30	120	na	10	47	23	76	20	13

^aGeometric mean. na: not available.

[†]Tumor location: R = rectum; S = sigmoid; RC = right colon; LC = left colon. Patients 5 and 8 had two tumors.

[‡]For circumferential tumors, volume = (10 \times the fraction of circumference) \times (height); for globular tumors, volume = (mean diameter)³.

[§]Mono-exponential functions have been fitted to time-activity curves in serum.

[¶]Bs-Mab activity-to-mulG activity ratio, determined from RIA.

^{**}Two-exponential functions have been fitted to time-radioactivity curves in serum. Vc = volume of the central compartment; Vss = distribution volume at the steady-state; Ftiss = fraction of the peripheral volume; Ta = half-life of the first exponential; Tb = half-life of the second exponential; MRTc = mean residence time in the central compartment; MRTb = mean residence time in whole body.

***Significantly different from tumor value, $p < 0.025$.

This RIA quantifies Bs-Mab only, since F6, but not 734, Mab has a kappa light chain and since 734, but not F6, Mab binds to In-DTPA solid phase.

Di-(In-DTPA)-TL was quantitated in urine by a two-step sandwich RIA using 734-IgG on the solid phase and as the tracer. The reference curve was obtained with serial dilutions of a purified Di-(In-DTPA)-TL in the urine of a healthy donor.

Indium-111 radioactivity was determined in 100 μ l of serum (5 min to 48 hr) and urine pools by counting in a gamma counter. Indium-111 complexes were analyzed by gel filtration chromatography on TSK 3000 SW column, equilibrated in phosphate-buffered saline (PBS) at 4°C, on 5 min, 5 hr, 24 hr and 48 hr serum samples and on urine pools. In some cases, samples were supplemented with In-DTPA complexes to a final concentration of 0.1 mM before chromatography. Sera sampled before Bs-Mab or hapten injection were supplemented in vitro with relevant amounts of Bs-Mab and/or labeled hapten (in order to mimic the composition of the 5-min sample) before chromatography.

Biodistribution was determined by weighing and counting biopsy specimens and a known volume of blood collected during surgery.

Immunohistochemistry was performed to assess CEA expression in tumor or normal colon cryostat sections (11).

Indium-111-labeled F(ab)₂ was infused into patients (1 mg in 100 ml of 0.9 g/liter NaCl). No adverse reaction was observed. Patients underwent surgery 1–4 days after injection. Biodistribution and immunohistochemistry studies were performed as above.

Pharmacokinetics Analysis

Bi-exponential curves were fitted to individual plasma radioactivity data corrected from the physical decay of the isotope (as fractions of injected activity (D) per liter) by nonlinear regression. All parameters were calculated according to Webster et al. (13) using zero-time activity (C0), area under time-activity curve (AUC), area under the time (time \times activity) curve (AUMC), mean residence time in the central compartment (MRTc = AUC/C0) and in whole-body (MRTb = AUMC/AUC), apparent volume of the central compartment (Vc = D/C0), apparent distribution volume at the steady state (Vss = D \times AUMC/AUC²) and the fraction of distribution in tissues (Ftiss = 1 – Vc/Vss). Mono-exponential curves were fitted to Bs-Mab activity data (It may be assumed that total muIgG or Bs-Mab concentration in serum and in interstitial fluids had reached a steady-state (14).) Fitted volume and half-life were defined as apparent distribution volume and elimination half-life, respectively (at the time of hapten injection).

Means and standard deviations are geometric or as otherwise indicated. Significant differences were tested using Student's t-test with the assumption of Log-normal distributions (15).

Correlation Analysis

To depict the influence of variations of experimental conditions on pharmacokinetics, biodistribution and image sensitivity, multiple linear regression analysis (15) was performed as follows: experimental conditions were described by five "independent" parameters (Xn): tumor volume, patient body weight, Bs-Mab ID, the time interval between injections and hapten ID. The individual values of these parameters (Xn_i) and the observed variable (Y_i, e.g., uptake by the tumor) were first normalized with respect to their mean value Xn or Y: x_n_i (or y_i) = Log (Xn_i/Xn) or Log (Y_i/Y). Then, the regression slopes (of y_i as a function of x_n_i), their s.d. and correlation coefficients (r²) were estimated using Symphony software (Lotus Development Corporation, Cambridge, MA). The regression slopes were considered as significant if different

from 0 within the 95% or 90% confidence interval (Student's t-test).

RESULTS

Quality of the Reagents

In terms of molecular weight (100 KDa), Bs-Mab was estimated as 77.5% \pm 2.5% pure by HPLC gel filtration analysis. Contaminants were essentially higher molecular weight conjugates and unconjugated Fab or Fab'. Immunoreactivity of ¹²⁵I-labeled Bs-Mab to In-DTPA, F6 anti-idiotypic Mab and COLO-205 (CEA positive) cells was 55% \pm 1%, 90% \pm 5% and 85% \pm 15%, respectively.

Unlabeled di-DTPA-TL was found to be more than 95% pure. For all patients, the ¹¹¹In immunoreactivity of the injected labeled hapten for 734 IgG was higher than 95%, except in the case of Patients 1 (84% \pm 1%) and 6 (90% \pm 1%). No loss of ¹¹¹In immunoreactivity was observed during 1 wk of storage in pH 5.0 buffer at either 4°C or 37°C (not shown).

No toxicity or adverse reactions were observed in patients.

Pharmacokinetics

MuIgG and Bs-Mab concentrations were obtained in patient serum after hapten injection. Both methods yielded well-correlated measurements (r² = 0.76). Fitted pharmacokinetic parameters are shown in Table 1.

Patient serum samples (5 min to 24 hr after hapten injection) were chromatographed by HPLC gel filtration to study the complexes of ¹¹¹In with serum protein. Serial chromatograms are shown in Figure 1. The molecular weight of the complexes are compatible with those expected of bivalent hapten complexes with either one Bs-Mab (100 KDa), or with two Bs-Mab (200 KDa), or, for Patients 2, 4 and 11, with other undefined serum proteins (>200 KDa). Free labeled hapten was not observed, except in the 5-min serum of Patient 6. After addition of excess unlabeled In-DTPA, more than 90% of the radioactivity was recovered in the free labeled hapten peak. The chromatography profile of 5-min sera could be mimicked in vitro by supplementing reference sera (without Bs-Mab) with adequate amounts of Bs-Mab and labeled hapten (that measured in 5-min samples), or sera before hapten injection (with Bs-Mab) with adequate amounts of labeled hapten (Fig. 1B). This suggests that: (1) complexes are the result of the specific binding of ¹¹¹In-di-(In-DTPA)-TL to circulating Bs-Mab; (2) higher molecular weight complexes are the result of Bs-Mab binding to other human proteins, probably pre-existing HAMA; and (3) transchelation of ¹¹¹In to plasma proteins, if any, remains low.

Table 1 also shows that 57% of injected ¹¹¹In was recovered in the urine 24 hr after injection. Urine radioactivity, on gel filtration chromatograms, was consistently associated with low molecular weight compounds (such as the ¹¹¹In-di-(In-DTPA)-TL). The mean immunoreactivity of ¹¹¹In recovered in the 0–5 hr urine pool was 91% \pm 3.5%, and 94% \pm 3.6% in the 5–24 hr pool (means of 11 patients).

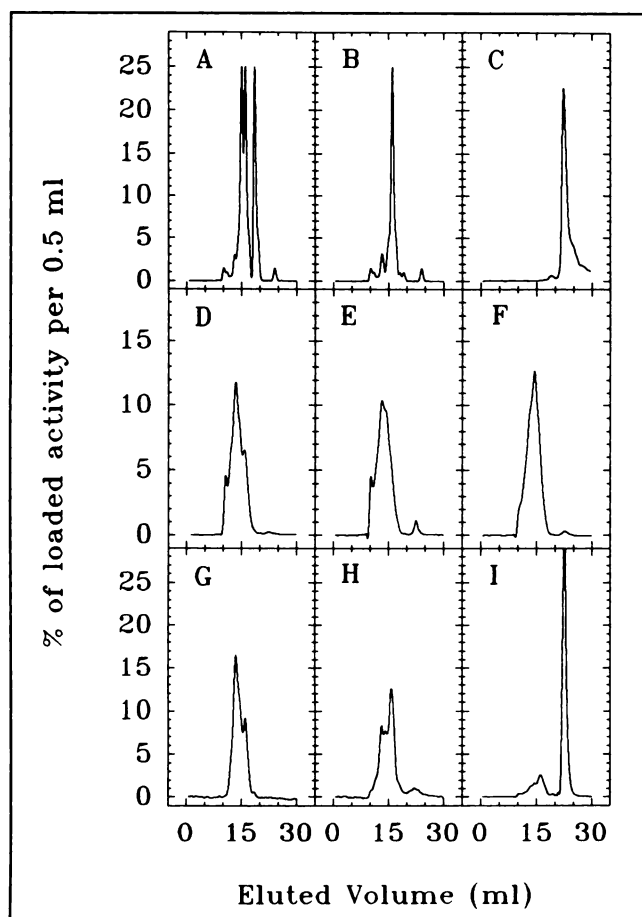


FIGURE 1. Gel filtration (see Material and Methods) analysis of serum of Patient 1. Optical density profiles after loading 100 μ l of (A) a calibration mixture (IgG, F(ab)₂ and Fab, 1 mg/ml) in PBS; (B) Bs-Mab (0.9 mg/ml) in PBS. (C) Radioactivity profiles after loading 100 liters of serum collected before Bs-Mab injection supplemented with ¹¹¹In-di-(In-DTPA)-TL (0.3 nM final); (D) 5-min serum; (E) 5-hr serum; (F) 24-hr serum; (G) serum collected before Bs-Mab injection supplemented with ¹¹¹In-di-(In-DTPA)-TL (0.3 nM final) in Bs-Mab (2 nM final); (H) serum collected before hapten injection supplemented with ¹¹¹In-di-(In-DTPA)-TL (0.3 nM final); and (I) 5 min serum after overnight incubation with excess In-DTPA (0.1 nM final).

The total amount of bivalent In-DTPA hapten recovered in the 0–5 hr urine pools was quantitated for Patients 3 to 7, and compared to the amount of labeled hapten recovered, estimated on the basis of the radioactivity measurement and of the specific activity of the injected hapten. The arithmetic mean ratio (measured/estimated) obtained was 1.52 ± 0.56 . Indium-111 leakage from di-(DTPA)-TL, if unlikely in plasma (see above), probably occurred in kidneys.

Biodistribution

Biodistribution data obtained from the determination of tissue radioactivity two days after injection of ¹¹¹In-di-(In-DTPA)-TL (Table 1) show the selectivity of hapten localization in tumors, as compared to all tissues tested.

When compared to the biodistribution data obtained 1–4 days after the injection of ¹¹¹In-labeled F6 F(ab)₂ (Table 2), uptake by the tumor and normal colon were not significantly lower; muscle, blood and liver activity were significantly decreased; and UR with respect to blood and liver were significantly increased (Table 1).

Imaging

A typical whole-body distribution pattern of ¹¹¹In 24 hr after hapten injection is shown in Figure 2. Circulating activity was generally not visible at 4 hr (at high Bs-Mab doses, it was faintly visible but disappeared at Day 1), in agreement with hapten pharmacokinetic data. Urinary bladder exhibited high activity (often occulting rectal lesions) but activity disappeared at Day 1. Moderate retention of ¹¹¹In was always observed in the kidney and sometimes in the liver and in the normal colon. Testis, salivary glands and rhinopharynx were labeled transiently.

Figure 3 shows scintigraphic images obtained in three typical cases, illustrating the quality of tumor delineation by SPECT; impairment by urinary bladder activity is apparent, especially in patients who received low Bs-Mab ID (Patients 2 and 3).

TABLE 2
Biodistribution (%ID/kg or %ID/liter) and Uptake Ratios of ¹¹¹In-Labeled F6 F(ab)₂ in Surgical Samples

			Patient no.					
	Mean* s.d.	—x s.d.	1	2	3	4	5	6
Surgery day			1	2	2	3	3	4
Tumor	12.9	5.5–30.2	33.1	15.7	11.6	8.6	27.6	3.2
Blood	3.1†	1.4–6.8	8.3	5.6	2.3	1.7	4.5	1.0
Colon	3.9	2.1–7.4	10.7	3.5	4.6	2.0	2.7	na
Liver	22.1†	10.2–47.9	18.4	13.1	na	14.3	69.1	na
Muscle	0.6†	0.3–1.0	0.7	1.3	0.6	0.4	0.6	0.3
Tumor/blood	4.2†	3.1–5.7	4.0	2.8	5.1	5.0	6.2	3.1
Tumor/colon	4.3	2.5–7.4	3.1	4.5	2.5	4.2	10.2	na
Tumor/liver	0.8†	0.4–1.7	1.8	1.2	na	0.6	0.4	na
Tumor/muscle	21.7	11.6–40.4	46	12	20	19	45	11

*Geometric mean. na = not available.

†Significantly different from paired Table 1 values, $p < 0.1$.

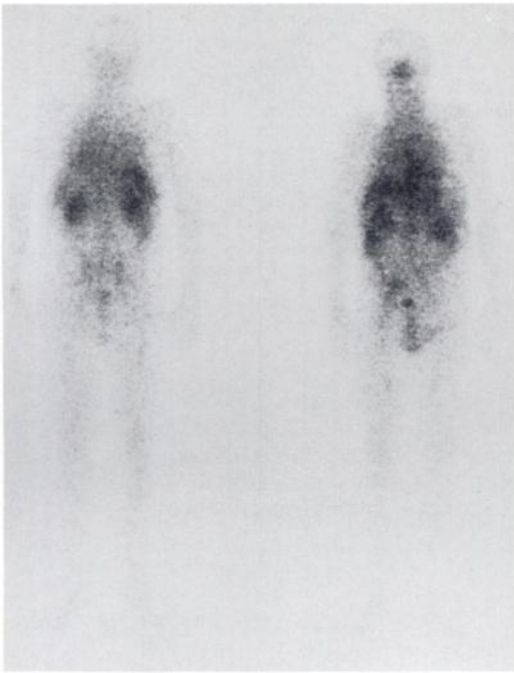


FIGURE 2. Anterior (right) and posterior (left) whole-body scan of Patient 5 one day after hapten injection.

Table 3 shows imaging efficacy of static and tomographic acquisitions, 4 and 24 hr after hapten injection. Tumors could be detected at 4 hr or 24 hr after hapten injection on static or tomographic views. The detection score increased with time, essentially because the radioactivity of urinary bladder disappeared. However, even at Day 1, tomography was necessary to obtain unequivocal (4/11) or high quality (5/11) images. In one case (Patient 3), the urinary bladder still interfered with the delineation of a rectal tumor at Day 1, and in another case (Patient 1), the tumor was not detected despite its good hapten uptake (Table 1).

Anti-Bs-Mab Immune Response

Results are summed and shown in Table 4. The anti-Bs-Mab RIA, showed no background with reference sera, and was much more specific than the RIA based on the use of anti-isotype. However, both RIA correlated if the elicited values were compared with basal values (16).

HAMA response of G (five patients) or M (two patients) isotype was detected. HAMA binding to Bs-Mab was efficiently completed by an excess of a mixture of F6 and 734 separate Fab, but was not completed by a mixture of another kappa, γ_1 Fab and of another lambda, γ_1 Fab. This

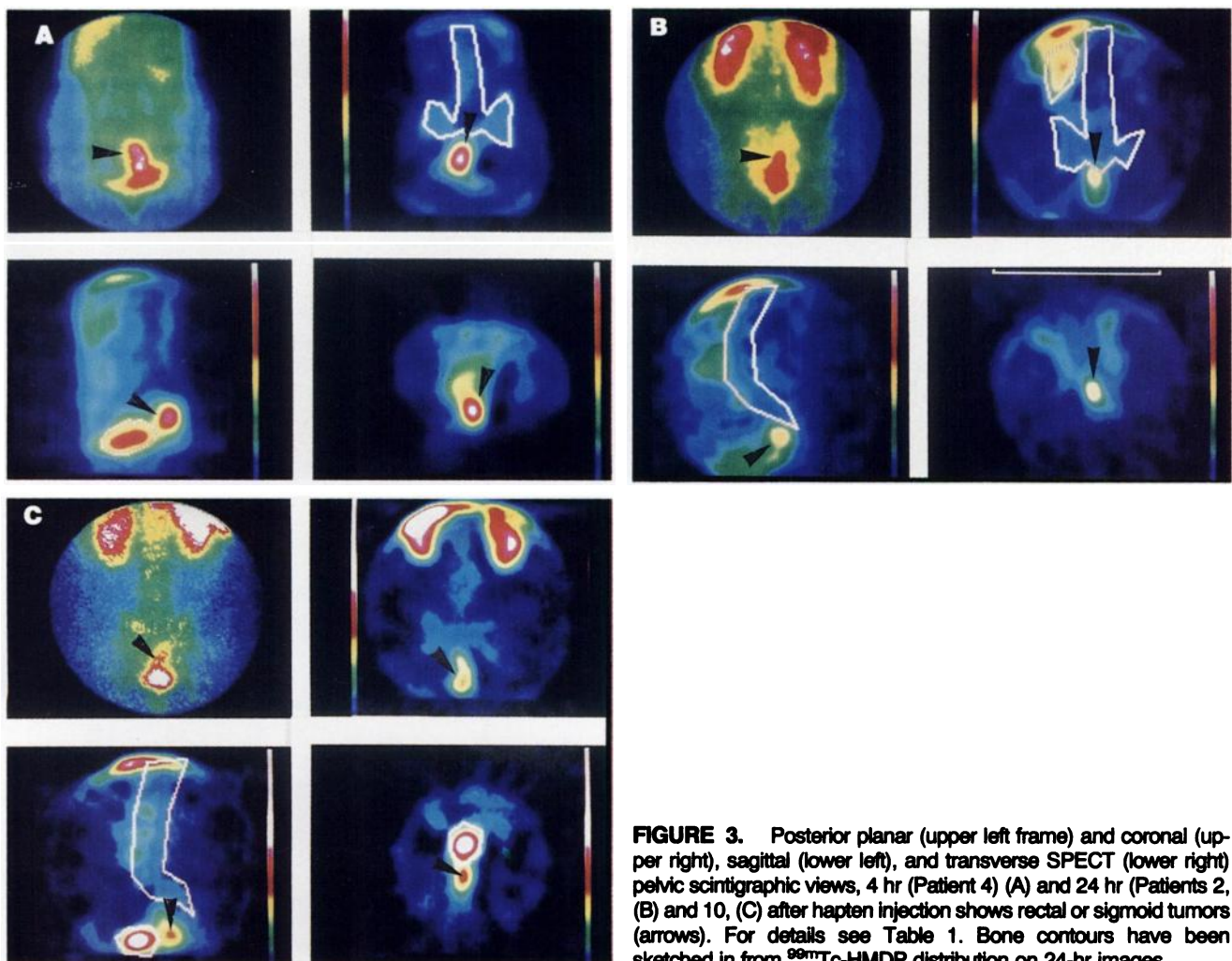


FIGURE 3. Posterior planar (upper left frame) and coronal (upper right), sagittal (lower left), and transverse SPECT (lower right) pelvic scintigraphic views, 4 hr (Patient 4) (A) and 24 hr (Patients 2, (B) and 10, (C) after hapten injection shows rectal or sigmoid tumors (arrows). For details see Table 1. Bone contours have been sketched in from ^{99m}Tc -HMDP distribution on 24-hr images.

TABLE 3
Sensitivity of Two-Step Immunoscintigraphy

	Time of acquisition	Patient no.											%*	% b.a. [†]
		1	2	3	4	5	6	7	8	9	10	11		
Planar anterior*	5 hr	—			+	+/+		+					31	62
Planar posterior		—			+	-/+		+			+		31	54
Tomography		—			+++	+++/>++	++	+		+++	++		54	31
Planar anterior	24 hr	—			+++	+++/>++	+	+	-/-	+		+	54	23
Planar posterior		—	+		+++	-/-	+	++	+/+	+	+	+	69	8
Tomography		—	++	+	+++	+++/>+++	++	+++	+++/>++	+++	++	++	92	0
Imaging score*		0	3	1	14	9	6	9	3	8	6	4		

*Images were scored as follows: (—) when tumor was not distinguishable from background, (bladder artifact, b.a.) when urinary bladder hampered visualization; (+) when the tumor was distinguishable from background but delineation was impossible due to the vicinity of another identifiable hot spot; (++) when other identifiable hot spots were more intensely labeled than the tumor but did not impair its delineation; and (+++) when tumor was the most intensely labeled area. For tomography, these criteria must be met for coronal, sagittal and transversal views. Quantitative scoring was obtained at 4 hr and 24 hr from the qualitative scale by adding (+) and subtracting (—) for static and tomographic views.

[†]b.a. or empty cells; bladder artifact.

suggests that HAMA was directed against the variable regions of F6 and/or 734 Fab and not against the maleimide-thiol chemical linker between the two fragments. In addition, pre-existing IgG or IgM HAMA were detected before Bs-Mab injection in three patients.

Correlation Analysis

The trends in the influence of patient characteristics and of injection parameters on measured variables were analyzed by multiple linear regression. Significant correlation coefficients reported in Table 5 can be interpreted as follows.

Tumor Volume. As expected, larger tumors were more easily detected. Interestingly, hapten pharmacokinetics, biodistribution, and tumor uptake (in %ID/kg) were not found correlated to this parameter. The influence of tumor size on Bs-Mab pharmacokinetics may be the result of unknown interactions in mIgG and Bs-Mab RIA.

Body Weight. As expected from a dilution effect, the concentration of Bs-Mab recovered in the serum of heavy patients at the time of hapten injection was lower. More hapten was recovered in the urine and less ¹¹¹In was re-

TABLE 4
Patient Anti-Bs-Mab Immune Response

		Patient no.											
		1	2	3	4	5	6	7	8	9	10	11	
Anti-Bs-Mab HAMA*	Before [†]	—	—	—	—	—	—	—	—	—	—	—	0/11
	Early	—	++	++	—	—	—	+	nd	++	+	+++	6/10
	Late	+	++	++	—	—	—	nd	—	+++	+++	++	6/10
IgG	Before	—	++	+	—	+	—	—	+	+	—	++	2/11
	Early	++	++		+	+	—	++	nd	+++	++	+++	4/9
	Late	++	+++	+++	+	++	+	nd	++	+++	+++	+++	4/10
IgM	Before	—	—	+	++	—	+	—	—	+	—	—	1/11
	Early	+	++		++	+	+	—	nd	++	+	++	2/10
	Late	+	++	+	++	+	+	nd	—	++	+	++	2/10
% Displacement	Bs-Mab		80	85	85				nd	95	95	85	
	F6-Fab'		35	20	65				nd	50	50	50	
	734-Fab		65	70	40				nd	70	45	35	
	F6-Fab' + 734 Fab		95	85	95				nd	95	95	75	
	Irrelevant IgG1	<10	<10	<10					nd	<10	<10	<10	
Pre-existing HAMA				IgG		IgM						IgG	3/11
Elicited HAMA			IgG	IgM	IgG			IgG		IgG	IgG	IgM	7/11

*Tests are described in Material and Methods. GAMIG-equivalent titers of anti-Bs-Mab were expressed on the following qualitative scale (in ng/ml): — < 60 < + < 250 < ++ < 1000 < +++. Samples before Bs-Mab injection are positive if (++) more than control serum; samples after Bs-Mab injection are positive if (++) more than before. nd: not done.

[†]Before: before Bs-Mab injection; early: 20 ± 10 days, and late: 60 ± 20 days after Bs-Mab injection.

TABLE 5
Influence of Protocol Parameters on Measured Variables*

Variables/parameters	Tumor volume	Body weight	Bs-Mab ID	Delay [†]	Hapten ID	R ²
MuIgG in serum	+0.17	-0.65	+1.02	-1.01	+0.71	0.87
Bs-Mab in serum	+0.13	-0.98	+1.16	-1.33	+0.47	0.92
MuIgG distribution volume	-0.51	—	-0.83	+1.13	-1.30	0.70
Bs-Mab distribution volume	—	—	—	—	—	0.56
Mouse IgG half-life	-0.22	—	-0.58	+1.03	-0.37	0.82
Bs-Mab half-life	-0.32	—	-0.87	—	—	0.60
Bs-Mab per MuIgG	—	—	—	—	—	0.28
Vc [‡]	-0.02	-0.12	-0.28	+0.32	-0.09	0.93
Vss	—	—	-0.53	+0.69	—	0.89
Ftiss	—	—	-0.24	+0.33	+0.24	0.84
Ta	-0.09	—	—	—	—	0.27
Tb	-0.05	—	+0.28	—	—	0.79
MRTp	—	-0.31	+0.58	-0.42	—	0.81
MRTb	—	—	+0.32	—	—	0.78
Urine recovery after 24 hr	—	+0.47	-0.27	—	—	0.56
Tumor	—	-2.67	+0.79	—	-1.22	0.85
Blood	—	-1.13	+0.77	—	-1.58	0.80
Colon	—	-1.78	+1.11	-1.01	—	0.94
Liver	—	—	+0.44	—	—	0.36
Muscle	—	-1.54	+0.80	—	—	0.74
Tumor/blood	—	-1.54	—	—	—	0.51
Tumor/colon	—	-0.83	—	+0.67	—	0.51
Tumor/liver	—	-2.41	—	—	-1.21	0.71
Tumor/muscle	—	-1.09	—	—	—	0.35
Imaging score	+1.50	-8.28	+1.98	—	+2.97	0.79

*Multiple linear regression analysis of Table 1 variables versus parameters (for details see Material and Methods). Regression slopes different from 0 within a 95% (resp 90%) confidence interval are indicated in bold (resp. normal); — = not significant. The slope must be interpreted as in the following example: increasing the mean Bs-Mab ID (3.1 mg, Table 1) of 10%, while other parameters stay at their mean value, will result in a relative variation of the mean tumor uptake (5.6% ID/kg, Table 1) equal to $+0.79 \times 10\% = +7.9\%$. This is of course true for small variations only.

[†]Time interval between Bs-Mab and hapten injection.

[‡]For symbols see Table 1.

covered in tissues (liver excepted) at surgery, especially in the tumor (UR were also lower). This could explain, together with more photon absorption through heavy patient body, that tumors were more difficult to detect in these patients.

Bs-Mab ID. As expected, Bs-Mab concentration recovered in patient serum at the time of hapten injection increased with Bs-Mab ID. Besides, increasing Bs-Mab ID decreased its distribution volume and its half-life. This has already been reported (17). It also decreased hapten extravasation (Vc, Vss and Ftiss) and elimination (recovery in urine). It increased hapten residence times (MRTc and MRTb) and T_b. It also increased ¹¹¹In recovery in tissues and imaging score, but did not influence UR.

Time Interval Between Bs-Mab and Hapten Injection. Increasing this parameter logically decreased Bs-Mab concentration in plasma while increasing its distribution volume. It also increased hapten extravasation. Increasing intervals significantly decreased the uptake of the hapten by the colon and increased tumor-to-colon UR. It had no influence on the uptake of ¹¹¹In by the tumor, on imaging score and on the ratio Bs-Mab per muIgG. This last point confirms the stability of the Bs-Mab in time.

Hapten ID. This parameter significantly influenced Bs-Mab pharmacokinetics, probably because the hapten could interfere with the RIA used to measure Bs-Mab concentration. Increasing hapten ID increased the fraction of hapten distributed in tissues (Ftiss). It had opposite effect on the recovery of ¹¹¹In in the tumor and in the blood at the time of surgery. However, it was beneficial for imaging.

DISCUSSION

Chemical recombination of anti-CEA and anti-In-DTPA Mab fragments, using a maleimide/N-hydroxy-succinimide cross-linking agent provided us with a homogeneous, immunoreactive (for both CEA and In-DTPA) and stable (in vitro and in vivo, (18)) Bs-Mab. This Bs-Mab could be injected safely into patients but induced HAMA in 7/11, as already reported with murine Mabs and fragments (16). The analysis of HAMA specificity showed no response against the chemical linker. However the relatively high response rate may be attributed to a small percentage of HMW conjugates. Its pharmacokinetics were found to be close to that of a conventional muIgG₁ F(ab')₂ (19).

Fully immunoreactive ¹¹¹In-labeled In-DTPA dimer could be reproducibly obtained. It was excreted in urine in

an essentially unmodified form (labeled, immunoreactive and bivalent). No leakage of the radioisotope was detected in plasma in accordance with the good stability of ^{111}In -DTPA chelates in serum (20).

After injection, the bivalent hapten was partially trapped by circulating Bs-Mab (Fig. 1). On the basis of ^{111}In -DTPA pharmacokinetics in humans (21), free hapten extravasation probably occurred in minutes and could not be detected using our sampling schedule. Complexed hapten may also be extravasated as such (T_a , with a mean value of 29 min, is probably characteristic for this phenomenon) or be dissociated and/or eliminated (probable characteristic half-life: T_b , mean value of 19 hr). As expected, these complexes, lacking Fc, were not precipitated by the reticulo-endothelial system (22). With hapten excess over Bs-Mab concentration in the plasma (Table 1, patients no. 2, 3, 7 and 8), most of the injected hapten remained free: V_{ss} was close to the total noncell water volume, $250 \pm 20 \text{ ml/kg}$ (23). Similarly, hapten T_b , MRTc and MRTb could be shortened mainly by decreasing Bs-Mab ID (Table 5). These pharmacokinetic properties are compatible with models developed by Jain et al. (24,25). Interestingly, the mean hapten T_b (or MRTb) was significantly lower than the half-life of the Bs-Mab itself ($p < 0.005$ with mIgG RIA and $p < 0.025$ using the Bs-Mab RIA), and of already reported plasma half-lives of murine (65 hr (13)) or chimeric (100 hr (26)) IgG, murine F(ab)_2 (36 hr (19)) and Fab' (35 hr (27)) in the human.

In spite of its reduced biodisponibility, hapten was taken up by the tumors with an efficiency comparable to that of ^{111}In -F6 F(ab)_2 (especially with a 5-mg Bs-Mab ID). This is an important point because preliminary two-step targeting clinical studies in which monovalent haptens were used (5) indicated that targeting efficiency was dramatically reduced when using Bs-Mab ID below 10 mg. This confirms that use of bivalent haptens was also beneficial in humans, as it was in animal models (4). As expected, hapten uptake by the tumor could be elevated by increasing the Bs-Mab ID, while increasing the hapten ID had the opposite effect, probably by saturating anti-hapten sites available in the tumor.

Conversely, the wider distribution and the accelerated clearance of the hapten (when compared to F(ab)_2) led to a general decrease in the radioactivity associated with normal tissues, and improved UR. In addition, ^{111}In uptake by the liver was reduced eleven-fold; the Bs-Mab catabolized by the liver (as conventional F(ab)_2 (11,19)) was obviously no longer available for hapten binding at the time of hapten injection. This hapten uptake by the liver, being poorly correlated with injection parameters (Table 5), may be the result of hapten: Bs-Mab complex "precipitation" in the reticulo-endothelial system (28) by pre-existing HAMA of a particular class or specificity. Alternatively, the Bs-Mab by itself may carry hapten into the liver and induce the subsequent sequestration of ^{111}In . The same phenomena probably occurred in the kidneys, which is the second major catabolizing organ for F(ab)_2 (14). Indeed, images

show that kidney activity was of the same order of magnitude as liver activity 4 hr (Fig. 3, Patient 4) and 24 hr (Fig. 2) after hapten injection.

The biodistribution of the hapten is in many aspects comparable to that reported with three step targeting using sequential injections of biotinylated anti-CEA Mab, avidin and ^{111}In -labeled biotin (29). With the hapten:anti-hapten Bs-Mab system, similar clearance of circulating Mab before hapten injection might be achieved by injecting polymerized hapten (provided that Bs-Mab contains Fc, in order to induce the precipitation of the complexes in the liver), as shown by Goodwin et al. (7). However, in these two techniques, preventing HAMA response will probably be a challenge.

When considered as an immunoscintigraphy technique, Bs-Mab-mediated targeting of ^{111}In -bivalent hapten could be advantageously compared to the use of ^{111}In -labeled F(ab)_2 and IgG (30), providing highly reduced liver activity, lower blood pool and background activity but more urinary bladder artifacts; tumors were more easily delineated, often without the need of image processing. Further optimization of image quality will be probably achieved by using at least 0.1 mg/kg of Bs-Mab (high tumor uptake) and higher hapten ID (rapid hapten extravasation); by reducing bladder activity thanks to a better patient management; and by decreasing the residual ^{111}In retention in liver and kidneys by using tracers labeled with ^{99m}Tc or ^{123}I (more labile from cells in which they may be trapped, (31)).

However, contrast improvement and its probable clinical usefulness still remain to be demonstrated in the case of the detection of recurrences and metastases. In the meantime, improved contrast may permit the detection of liver metastasis, even with ^{111}In as an isotope (32), as well as radioimmunoguided surgery (33,34).

ACKNOWLEDGMENTS

The authors thank J. P. Mach for helpful discussions and G. Anfos, C. Curtet, R. Cheballah, P. Meyer, P. Peltier and H. Rickenberg who gave their enthusiastic intellectual or technical support.

REFERENCES

1. Reardan DT, Meares CF, Goodwin DA, et al. Antibodies against metal chelates. *Nature* 1985;316:265-268.
2. Goodwin DA, Meares CF, McCall MJ, McTigue M, Chaovapong W. Pretargeted immunoscintigraphy of murine tumors with indium-111-labeled bifunctional haptens. *J Nucl Med* 1988;29:226-234.
3. Gridley DS, Ewart KL, Cao JD, Stickney DR. Hyperthermia enhances localization of ^{111}In -labeled hapten to bifunctional antibody in human colon tumor xenografts. *Cancer Res* 1991;51:1515-1520.
4. Le Doussal JM, Gruaz-Guyon A, Martin M, Gautherot E, Delaage M, Barbet J. Targeting of indium-111-labeled bivalent hapten to human melanoma mediated by bispecific monoclonal antibody conjugates: imaging of tumors hosted in nude mice. *Cancer Res* 1990;50:3445-3452.
5. Stickney DR, Slater JB, Kirk GA, Ahlem C, Chang CH, Frincke JM. Bifunctional antibody: ZCE/CHA ^{111}In BLEDTA-IV clinical imaging in colorectal carcinoma. *Antibody Immunconj Radiopharm* 1989;2:1-13.
6. Le Doussal JM, Martin M, Gautherot E, Delaage M, Barbet J. In vitro and in vivo targeting of radiolabeled monovalent and bivalent haptens with dual specificity monoclonal antibody conjugates: enhanced bivalent hapten affinity for cell-bound antibody conjugate. *J Nucl Med* 1989;30:1358-1366.
7. Goodwin DA, Meares CF, McTigue M, et al. Pretargeted immunoscintig-

- raphy: effect of hapten valency on murine tumor uptake. *J Nucl Med* 1992;33:2006–2013.
8. Le Doussal JM, Gautherot E, Martin M, Barbet J, Delaage M. Enhanced in vivo targeting of an asymmetric bivalent hapten to double-antigen-positive mouse B cells with monoclonal antibody conjugate cocktails. *J Immunol* 1991;146:169–175.
9. Le Doussal JM, Gautherot E, Martin M, Delaage M, Barbet J. Affinity enhanced targeting of radiolabeled divalent haptens to human melanoma in nude mice [Abstract]. *J Nucl Med* 1989;30:907.
10. Hnatowitch DJ, Childs RL, Lanteigne D. The preparation of DTPA-coupled antibodies radiolabeled with metallic radionuclides: an improved method. *J Immunol Methods* 1983;65:147–157.
11. Chetanneau A, Baum RP, Lehur PA, et al. Multi-centre immunoscintigraphic study using indium-111-labeled CEA-specific and/or 19-9 monoclonal antibody F(ab)₂ fragments. *Eur J Nucl Med* 1990;17:223–229.
12. Meares CF, McCall MJ, Reardan DT, Goodwin DA, Diamanti CI, McTigue M. Conjugation of antibodies with bifunctional chelating agents: isothiocyanate and bromoacetamide reagents methods of analysis and subsequent addition of metal ions. *Anal Biochem* 1984;142:68–78.
13. Webster WB, Harwood SJ, Carroll RG, Morissey MA. Pharmacokinetics of indium-111-labeled B72.3 monoclonal antibody in colorectal cancer patients. *J Nucl Med* 1992;33:498–504.
14. Covell DG, Barbet J, Holton OD, Black CDV, Parker RJ, Weinstein JN. Pharmacokinetics of monoclonal immunoglobulin G₁, F(ab)₂ and Fab' in mice. *Cancer Res* 1986;46:3969–3878.
15. Snedecor GW, Cochran WG. In: *Statistical methods*. Ames, IA: Iowa State University Press, 1980:54–56.
16. Massuger LF, Thomas CM, Segers MF, et al. Specific and nonspecific immunoassay to detect HAMA after administration of Indium-111-labeled OV-TL3 F(ab)₂ monoclonal antibody to patients with ovarian cancer. *J Nucl Med* 1992;33:1958–1963.
17. Eger RR, Covell DG, Carrasquillo JA, et al. Kinetic model for the biodistribution of ¹¹¹In-labeled monoclonal antibody in humans. *Cancer Res* 1987;47:3328–3336.
18. Ghetie V, Till MA, Ghetie MA, et al. Preparation and characterization of conjugates of recombinant CD4 and deglycosylated ricin A chain using different cross-linkers. *Bioconj Chem* 1990;1:24–31.
19. Buraggi GL, Callegaro L, Mariani G, et al. Imaging with ¹³¹I-labeled monoclonal antibody to a high-molecular-weight melanoma-associated antigen in patients with melanoma: efficacy of whole immunoglobulin and its F(ab)₂ fragments. *Cancer Res* 1985;45:3378–3387.
20. Hnatowitch DJ, Griffin TW, Kosciuszky C, et al. Pharmacokinetics of an indium-111-labeled monoclonal antibody in cancer patients. *J Nucl Med* 1985;26:849–858.
21. Houston SA, Sampson WFD, MacLeod MA. A compartmental model for the distribution of In-113m-DTPA and Tc-99m(Sn)DTPA in man following intravenous injection. *Int J Nucl Med Biol* 1979;6:85–95.
22. Clarkson SB, Kimberly RP, Valinski JF, et al. Blockade of clearance of immune complexes by an anti-Fcγ receptor monoclonal antibody. *J Exp Med* 1986;164:474–489.
23. Blacque Belair A, Mathieu de Fossey B, Fourestier M. In: *Dictionnaire des constantes biologiques et physiques*. Paris, France: Maloine S.A.; 1980: 163–167.
24. Yuan F, Baxter LT, Jain RK. Pharmacokinetic analysis of two-step approaches using bifunctional and enzyme-conjugated antibodies. *Cancer Res* 1991;51:3119–3130.
25. Baxter LT, Yuan F, Jain RK. Pharmacokinetics analysis of the perivascular distribution of bifunctional antibodies and haptens: comparison with experimental data. *Cancer Res* 1992;52:5838–5844.
26. Meredith RF, LoBuglio AF, Plott WE, et al. Pharmacokinetics, immune response and biodistribution of ¹³¹I-labeled chimeric mouse/human IgG1,k 17-1A monoclonal antibody. *J Nucl Med* 1991;32:1162–1168.
27. Larson SM, Carrasquillo JA, Krohn KA, et al. Localization of ¹³¹I-labeled p97-specific Fab fragments in human melanoma as a basis for radiotherapy. *J Clin Invest* 1983;72:2101–2114.
28. Benacerraf B, Sebestyen M, Copper NS. The clearance of antigen antibody complexes from the blood by the reticulo-endothelial system. *J Immunol* 1959;82:131–137.
29. Paganelli G, Magnani P, Zito F, et al. Three-step monoclonal antibody tumor targeting in carcinoembryonic antigen-positive patients. *Cancer Res* 1991;51:5960–5966.
30. Doerr RJ, Abdel-Nabi H, Baker JM, Steinberg S. Detection of primary colorectal cancer with indium-111 monoclonal antibody B72.3. *Arch Surg* 1990;125:1601–1605.
31. Naruki Y, Carrasquillo JA, Reynolds JC, et al. Differential cellular catabolism of ¹¹¹In, ⁹⁰Y and ¹²⁵I-labeled T101 anti-CD5 monoclonal antibody. *Int J Radiat Appl Instrum* 1990;17:201–207.
32. Bischof-Delaloye A, Delaloye B, Buchegger F, et al. Clinical value of immunoscintigraphy in colorectal carcinoma patients: a prospective study. *J Nucl Med* 1989;30:1646–1656.
33. Martin DT, Hinkle GH, Tuttle S, et al. Intraoperative radioimmunodetection of colorectal cancer with a hand held radiation detector. *Am J Surg* 1985;150:672–676.
34. Curtet C, Vuillez JP, Daniel G, et al. Feasibility study of radioimmunoguided surgery of colorectal carcinomas using indium-111 CEA-specific monoclonal antibody. *Eur J Nucl Med* 1990;17:299–304.